Differential regulation of symmetry genes and the evolution of floral morphologies

Differential regulation of symmetry genes and the evolution of floral morphologies

Lena C. Hileman†, Elena M. Kramer, and David A. Baum‡

Department of Organismic and Evolutionary Biology, Harvard University, 16 Divinity Avenue, Cambridge, MA 02138

Communicated by John F. Doebley, University of Wisconsin, Madison, WI, September 5, 2003 (received for review July 16, 2003)

Shifts in flower symmetry have occurred frequently during the diversification of angiosperms, and it is thought that such shifts play important roles in plant–pollinator interactions. In the model developmental system *Antirrhinum majus* (snapdragon), the closely related genes *CYCLOIDEA* (*CYC*) and *DICHOTOMA* (*DICH*) are needed for the development of zygomorphic flowers and the determination of adaxial (dorsal) identity of floral organs, including adaxial stamen abortion and asymmetry of adaxial petals. However, it is not known whether these genes played a role in the divergence of species differing in flower morphology and pollination mode. We compared *A. majus* with a close relative, *Mohavea confertiflora* (desert ghost flower), which differs from *Antirrhinum* in corolla (petal) symmetry and pollination mode. In addition, *Mohavea* has undergone a homeotic-like transformation in stamen number relative to *Antirrhinum*, aborting the lateral and adaxial stamens during flower development. Here we show that the patterns of expression of *CYC* and *DICH* orthologs have shifted in concert with changes in floral morphology. Specifically, lateral stamen abortion in *Mohavea* is correlated with an expansion of *CYC* and *DICH* expression, and internal symmetry of *Mohavea* adaxial petals is correlated with a reduction in *DICH* expression during petal differentiation. We propose that changes in the pattern of *CYC* and *DICH* expression have contributed to the derived flower morphology of *Mohavea* and may reflect adaptations to a pollination strategy resulting from a mimetic relationship, linking the genetic basis for morphological evolution to the ecological context in which the morphology arose.

evolution of development | floral evolution | *Mohavea* | *Antirrhinum* | *CYCLOIDEA*/*DICHOTOMA*

Much of extant flower diversity results from evolutionary changes in the shape and number of floral organs, but how such transitions have occurred during angiosperm evolution remains enigmatic. Developmental evolutionary biology aims to uncover the developmental and genetic mechanisms that result in morphological differences between species and to understand the evolutionary forces contributing to the origin of morphological novelties. One promising approach is to study closely related species to determine whether they differ in the expression of genes that, based on studies in model systems, could explain phenotypic differences between the species (1, 2). We focus here on the model system snapdragon (*Antirrhinum majus*) and the desert ghost flower (*Mohavea confertiflora*), two closely related species that show marked differences in flower development and morphology. In particular, we focus on the evolutionary transition in stamen number and petal morphology and explore the hypothesis that these shifts involve changes in the expression of floral symmetry genes.

All species of *Antirrhinum*, including the model species *A. majus* (snapdragon), produce flowers that are strongly bilaterally symmetrical (zygomorphic) (Fig. 1*b*) with distinct adaxial (dorsal), lateral, and abaxial (ventral) petals; they produce four mature stamens per flower because of the abortion of the fifth, adaxial stamen primordium during flower development (Fig. 1 *d* and *f*). Contributing to strong bilateral symmetry, the adaxial and lateral petals are internally asymmetrical with different patterns of growth occurring on either side of the midline (Fig. 1*h*). The two species of *Mohavea* have a floral morphology that is highly divergent from *Antirrhinum* (3), resulting in its traditional segregation as a distinct genus. *Mohavea* corollas, especially those of *M. confertiflora*, are superficially radially symmetrical (actinomorphic), mainly due to distal expansion of the corolla lobes (Fig. 1*a*) and a higher degree of internal petal symmetry relative to *Antirrhinum* (Fig. 1 *a* and *g*). During *Mohavea* flower development, the lateral stamens, in addition to the adaxial stamen, are aborted, resulting in just two stamens at flower maturity (Fig. 1 *c* and *e*). Nonetheless, contradicting the traditional taxonomy, molecular phylogenetic data indicate that *Mohavea* is nested within a tetraploid North American clade of *Antirrhinum*. Thus, *Mohavea*'s divergent floral morphology is derived from one similar to that of *A. majus* (Fig. 2; R. K. Oyama and D.A.B., unpublished data).

In *A. majus*, the genes *CYCLOIDEA* (*AmCYC*) and *DICHOTOMA* (*AmDICH*) determine adaxial identity of floral organs (4, 5). *dich* mutants display a mildly abaxialized phenotype with modifications to adaxial petal morphology and a wild-type pattern of stamen abortion. *cyc* mutants produce flowers that are strongly abaxialized and lack stamen abortion. Thus, partially symmetrical flowers develop in plants that carry mutations in either *AmCYC* or *AmDICH*, but the severity of this phenotype differs between the loci. Both *AmCYC* and *AmDICH* are necessary to determine adaxial flower identity, because *cyc dich* double mutants form fully abaxialized, radially symmetrical flowers lacking stamen abortion. The timing and localization of *AmCYC* and *AmDICH* expression is correlated with the mutant phenotypes. *AmCYC* is expressed across adaxial petals and in the adaxial staminode (aborted stamen), consistent with its expression being necessary for stamen abortion (5) (Fig. 3). *AmDICH* is also expressed in the adaxial staminode, but its expression in the adaxial petals is restricted to the inner half of each adaxial petal, the half closest to the medial line of flower symmetry (4) (Figs. 1*h* and 3). Because *dich* mutants produce more symmetrical adaxial petal lobes than wild type (4), the asymmetrical expression of *AmDICH* across the petals is thought to cause the internal asymmetry of adaxial petals (4), perhaps through a differential regulation of growth direction (6).

AmCYC and *AmDICH* are closely related members of the TCP (TB1, CYC, and PCFs) family of transcription factors, many of which influence meristem and primordium growth (7). Given that natural variation at TCP loci has been implicated in differences in floral form (8–11), and that their expression is necessary for stamen abortion and petal asymmetry in snapdragon (4, 5), we considered *CYC* and *DICH* to be ideal candidate genes for the evolution of floral novelties that distin-

Data deposition: The sequences reported in this article have been deposited in the GenBank database (accession nos. AF512687–AF512723).

†To whom correspondence should be addressed at: Department of Molecular Cellular and Developmental Biology, Yale University, P.O. Box 208104, New Haven, CT 06520. E-mail: lena.hileman@yale.edu.

‡Present address: Department of Botany, University of Wisconsin, 430 Lincoln Drive, Madison, WI 53706.

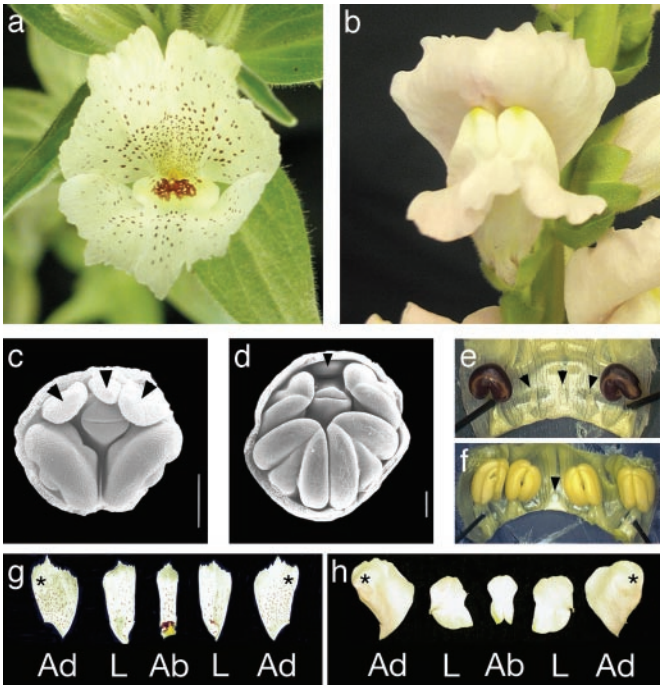

Fig. 1. (*a*) *Mohavea confertiflora* flower morphology showing superficial radial symmetry. (*b*) *Antirrhinum majus* flower morphology showing clear bilateral symmetry. (*c*) SEM of *M. confertiflora* early-stage flower with adaxial and lateral stamen primordia indicated. (*d*) SEM of *A. majus* early-stage flower with adaxial stamen primordium indicated (arrowheads). In *c* and *d*, petal and sepal tissues have been removed. (*e*) Dissected *M. confertiflora* flower showing aborted adaxial and lateral staminodes (arrowheads). (*f*) Dissected early stage *A. majus* flower showing aborted adaxial staminode (arrowhead). (*g* and *h*) Adaxial (Ad), lateral (L), and abaxial (Ab) petal lobes dissected from *M. confertiflora* and *A. majus*, respectively. *M. confertiflora* petal lobes show a higher degree of internal petal symmetry (*g*) when compared with *A. majus* petal lobes (*h*). Asterisks indicate the half of each adaxial petal that is adjacent to the medial line of corolla symmetry. Arrowheads indicate position of aborted stamens. (Scale bars, 0.2 mm.) *M. confertiflora* and *A. majus* SEMs courtesy of Peter K. Endress. [Reproduced with permission from ref. 3 (Copyright 1998, Society for Experimental Biology).]

guish *Mohavea* from *Antirrhinum* flowers. We hypothesized that lateral stamen abortion during *Mohavea* flower development is due to an expansion of *CYC* and/or *DICH* homologs into the

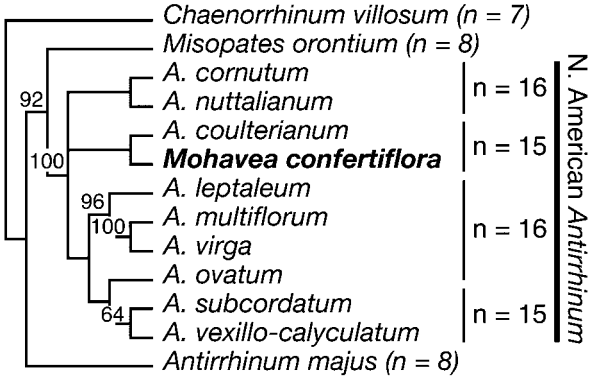

Fig. 2. Maximum likelihood estimate of relationships among *Antirrhinum* taxa and *Mohavea*. *Mohavea* is nested within the tetraploid clade of North American *Antirrhinum*. The tree is rooted with *CYC* and *DICH* sequences from *Chaenorrhinum villosum*. Maximum parsimony bootstrap values >50% are indicated above nodes. Ploidy levels are indicated to the right of taxa.

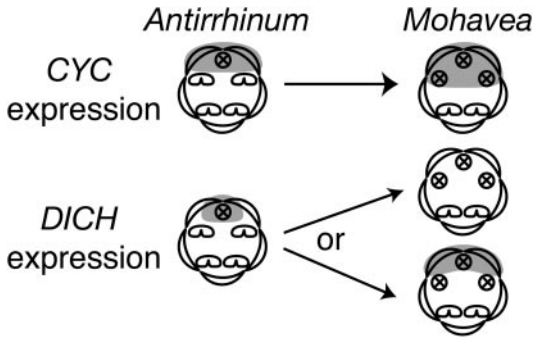

Fig. 3. *CYC* in *A. majus* is expressed across the adaxial petals and in the aborted adaxial staminode. This pattern of *CYC* expression determines adaxial petal identity and adaxial stamen abortion (5). Hypothesized expression in *Mohavea* is expanded such that the aborted lateral stamen primordia are also in the domain of *CYC* expression. *DICH* expression in the *A. majus* corolla is restricted to the inner half of each adaxial petal, the half closest to the medial line of symmetry. *DICH* expression in this domain results in internal asymmetry of dorsal petal lobes (4), putatively through differential regulation of growth direction (6). The hypothesized expression of *DICH* in *Mohavea* is either an expansion or a reduction across adaxial petals, correlating with the higher degree of internal symmetry observed in *Mohavea* dorsal petals. An expansion or reduction in *DICH* expression in *Mohavea* may result in more uniform growth directionality.

lateral staminodes and that the higher degree of internal petal symmetry in *Mohavea* adaxial petals is due to expansion or contraction of *DICH* expression, leading to uniform expression across these petals (Fig. 3).

Materials and Methods

Cloning of *CYC* and *DICH* Orthologs and Phylogenetic Analysis. PCR was used to amplify, clone, and sequence *CYC* and *DICH* orthologs from genomic DNA of *Antirrhinum cornutum*, *Antirrhinum coulterianum*, *Antirrhinum leptaleum*, *Antirrhinum multiflorum*, *Antirrhinum nuttalianum*, *Antirrhinum ovatum*, *Antirrhinum subcordatum*, *Antirrhinum vexillo-calyculatum*, *Antirrhinum virga*, and *Mohavea confertiflora* according to published methods (12). An additional forward primer, 5′-CACATACCTACATCTCCCTCAGG-3′, was used. The sequences reported here have been deposited in the GenBank database (accession nos.: *A. cornutum*, AF512687, AF512697, AF512716, and AF512706; *A. coulterianum*, AF512688, AF512698, AF512717, and AF512707; *A. leptaleum*, AF512689 and AF512708; *A. multiflorum*, AF512690, AF512699, AF512718, and AF512709; *A. nuttalianum*, AF512691, AF512700, AF512719, and AF512710; *A. ovatum*, AF512692, AF512701, AF512720, and AF512711; *A. subcordatum*, AF512693, AF512702, AF512721, and AF512712; *A. vexillo-calyculatum*, AF512695, AF512704, AF512722, and AF512714; *A. virga*, AF512694, AF512703, and AF512713; and *M. confertiflora*, AF512696, AF512705, AF512723, and AF512715). *CYC* and *DICH* sequences were aligned manually with reference to both nucleotide and hypothetical amino acid information.

To evaluate gene orthology, we conducted phylogenetic analysis of the isolated genes and published *CYC* and *DICH* sequences from *A. majus* (Y16313 and AF199465, respectively), *Chaenorrhinum villosum* (AF512601 and AF512591), and *Misopates orontium* (AF512600 and AF512594). *CYC* and *DICH* sequences were combined into a single matrix and analyzed together. Phylogenetic analyses were conducted by using PAUP*4.0b1 (16). We estimated the maximum likelihood tree by using a random taxon addition sequence, tree bisection reconnection heuristic search under the general time-reversible model of evolution with a discrete gamma model, allowing for four

categories of rate variation among sites (13, 14). Maximum parsimony bootstrap support for nodes (15) was estimated with 1,000 heuristic search replicates, random taxon addition, and the Tree Bisection and Reconnection branch-swapping algorithm.

RNA *in Situ* Hybridization. RNA *in situ* hybridization was performed according to described methods (17) with the following modifications: tissue fixation in FAA (50% EtOH/10% formalin/5% acetic acid/0.1% DMSO), probes were alkaline hydrolyzed to 400 bp, and, after signal development, tissues were counterstained with Calcofluor (0.002%). Digoxygenin-labeled probes of *McCYC1*, *McCYC2*, *McDICH1*, and *McDICH2* were prepared from linearized templates cloned into pCR4 plasmid (Invitrogen). RNA probes were gene-specific and included the coding region sequenced for each locus; this region corresponded to ≈94% and 95% of the coding sequence for *CYC* and *DICH* loci, respectively.

RT-PCR. Tissues used for RT-PCR consisted of floral organs dissected from relatively late-stage *M. confertiflora* flowers in which petal and stamen primordia had undergone a high degree of differentiation (Fig. 1*e*). Sepals were removed from the outer whorl. The corolla tube and petal lobes, including the attached abaxial stamens and lateral and adaxial staminodes of 110 flowers, were dissected into abaxial, lateral, and adaxial regions. Total RNA was extracted (18) from the tissues of the three corolla plus stamen/staminode regions and from the sepal tissues for RT-PCR experiments. RT-PCR was performed as described (18) by using locus-specific primers: *McCYC1* (forward 5′-GCTGCTACTTCGGTGGTC-3′, reverse 5′-AATGCCTCACGAGTACCC-3′), *McCYC2* (forward 5′-GCCGCTACGTCTGTTGTT-3′, reverse 5′-AACGCCTCGCGATTACCT-3′), *McDICH1* (forward 5′-CACGACGTGATTTCCGAG-3′, reverse 5′-GGACAGCGGTGAGTTTGC-3′) and *McDICH2* (forward 5′-CATGACGTGATTTCCGGC-3′, reverse 5′-CTTCATAATTAGTTGAGGGAC-3′). Primers that amplify actin were used as a positive control (19). RT-PCR products were cloned, and between 5 and 12 clones from each RT-PCR were sequenced to confirm locus-specificity.

Results

To test our hypothesis that lateral stamen abortion and internal petal symmetry in *Mohavea* are due to changes in the regulation of *CYC* and/or *DICH* homologs during flower development (Fig. 3), the *CYC* and *DICH* orthologs of *M. confertiflora* were cloned and sequenced. As with other *CYC* and *DICH* homologs, these sequences lacked introns in the coding regions. Phylogenetic analysis of the resultant sequences confirmed that two *CYC* loci (*McCYC1* and *McCYC2*) and two *DICH* loci (*McDICH1* and *McDICH2*) were isolated (data not shown). This result is expected because *Mohavea* is tetraploid relative to *A. majus* (ref. 20; Fig. 2). Apart from six to eight triplet in-frame indels, *McCYC* and *McDICH* loci share ≈94.4% and 92.0% nucleotide identity with *AmCYC* and *AmDICH*, respectively. RNA *in situ* hybridization and locus-specific RT-PCR were used to determine the spatial and temporal patterns of *McCYC* and *McDICH* gene expression in *M. confertiflora*.

RNA *in situ* hybridization in *M. confertiflora* revealed that *McCYC1* and *McCYC2* expression patterns are indistinguishable across all observed stages of flower development (Fig. 4 *a–d* and data not shown). Expression is first detected before the initiation of organ primordia, with RNA concentrated in the adaxial region of early floral meristems (Fig. 4*a*). Once sepal, petal, and stamen primordia have initiated, *McCYC1* and *McCYC2* expression differ markedly from that of *AmCYC*. *McCYC1* and *McCYC2* expression becomes concentrated in regions of the developing lateral and adaxial stamen primordia (Fig. 4 *b* and *c*). The expression in adaxial petals of *M. confertiflora* (Fig. 4 *b* and *c*) is similar to that observed for *AmCYC* (4). Therefore, it is specifically *McCYC* expression in lateral stamen primordia that differs from *CYC* expression in *A. majus*, correlating perfectly with the additional stamen abortion seen during *Mohavea* flower development.

McDICH1 and *McDICH2* differ in the timing of their expression. Transcripts of *McDICH1* first accumulate in the adaxial region of early floral meristems (Fig. 4*e*) in a similar pattern to *McCYC*, *AmCYC*, and *AmDICH*. In contrast, multiple hybridizations of *McDICH2* probed to similar stage flowers did not detect expression (Fig. 4*i*). After the initiation of sepal, petal, and stamen primordia, *McDICH1* and *McDICH2* are expressed in adaxial and lateral stamen primordia (Figs. 4 *f*, *g*, *j*, and *k*), with expression declining in later stages (Fig. 4*h*; data for *McDICH2* not shown). *McDICH1* and *McDICH2* expression differs markedly from *AmDICH* expression (4), and correlates with additional stamen abortion during *Mohavea* flower development.

In the corolla, *McDICH1* (Fig. 4*f*), but not *McDICH2* (Fig. 4*j*), is expressed in initiating petal primordia. However, neither *McDICH1* nor *McDICH2* expression is detected in petals during mid (Fig. 4 *g* and *k*) and later stages (Fig. 4*h*; data not shown for *McDICH2*, but similar to *McDICH1*, Fig. 4*h*) of flower development when petals undergo differentiation. This finding is significantly different from *A. majus* developing petals, where *AmDICH* is expressed in the inner region of each adaxial petal through petal differentiation, resulting in internal petal asymmetry (4). The lack of *McDICH* expression in *M. confertiflora* petal lobes by using *in situ* hybridization correlates with the higher degree of internal petal symmetry observed in *Mohavea* flowers.

Locus-specific RT-PCR results using dissected petal plus stamen/staminode tissue from relatively late-stage flowers that have undergone a high degree of differentiation (Fig. 1*e*) are in line with the observed *in situ* expression patterns. Expression of *McCYC1*, *McCYC2*, *McDICH1*, and *McDICH2* is observed in adaxial and lateral regions of dissected corolla plus staminode tissue (Fig. 5). By using *in situ* hybridization, expression of *McDICH1* and *McDICH2* was not detected during later stages of flower development. This discrepancy between the RT-PCR and *in situ* hybridization results likely reflects a higher sensitivity of RT-PCR to low levels of gene expression in later-stage flowers. The similarity in RT-PCR for *McCYC1* relative to *McCYC2*, and *McDICH1* relative to *McDICH2*, suggests that the similar patterns observed with *in situ* hybridization for the paralogous *McCYC* and *McDICH* loci are not entirely due to probe cross-reactivity.

Discussion

McCYC and *McDICH* expression in *M. confertiflora* fits the hypothesis that changes in the regulation of these flower-symmetry genes played a causal role in morphological evolution. Most notably, expression of *McCYC* and *McDICH* in lateral stamen primordia is correlated with their abortion during *Mohavea* flower development. Changes in *DICH* expression may correlate with differences in corolla morphology between *A. majus* and *M. confertiflora*. Unlike in *A. majus*, where medially restricted *AmDICH* expression in the adaxial petals results in petal-lobe asymmetry (4), *in situ* hybridization did not detect *McDICH* expression in *Mohavea* adaxial corollas at stages when petals undergo differentiation. However, the RT-PCR results show that *McDICH1* and *McDICH2* are expressed in the adaxial and lateral regions of later-stage flowers at levels that are apparently too low to be detected by *in situ* hybridization. Given that *in situ* hybridization shows *McDICH1* and *McDICH2* expression in staminodes but not petals at midstages of development (Fig. 4 *g* and *k*), the RT-PCR results likely reflect low levels of *McDICH* expression in the adaxial and lateral staminodes in late-stage flowers. If *McDICH* is expressed in the medial region

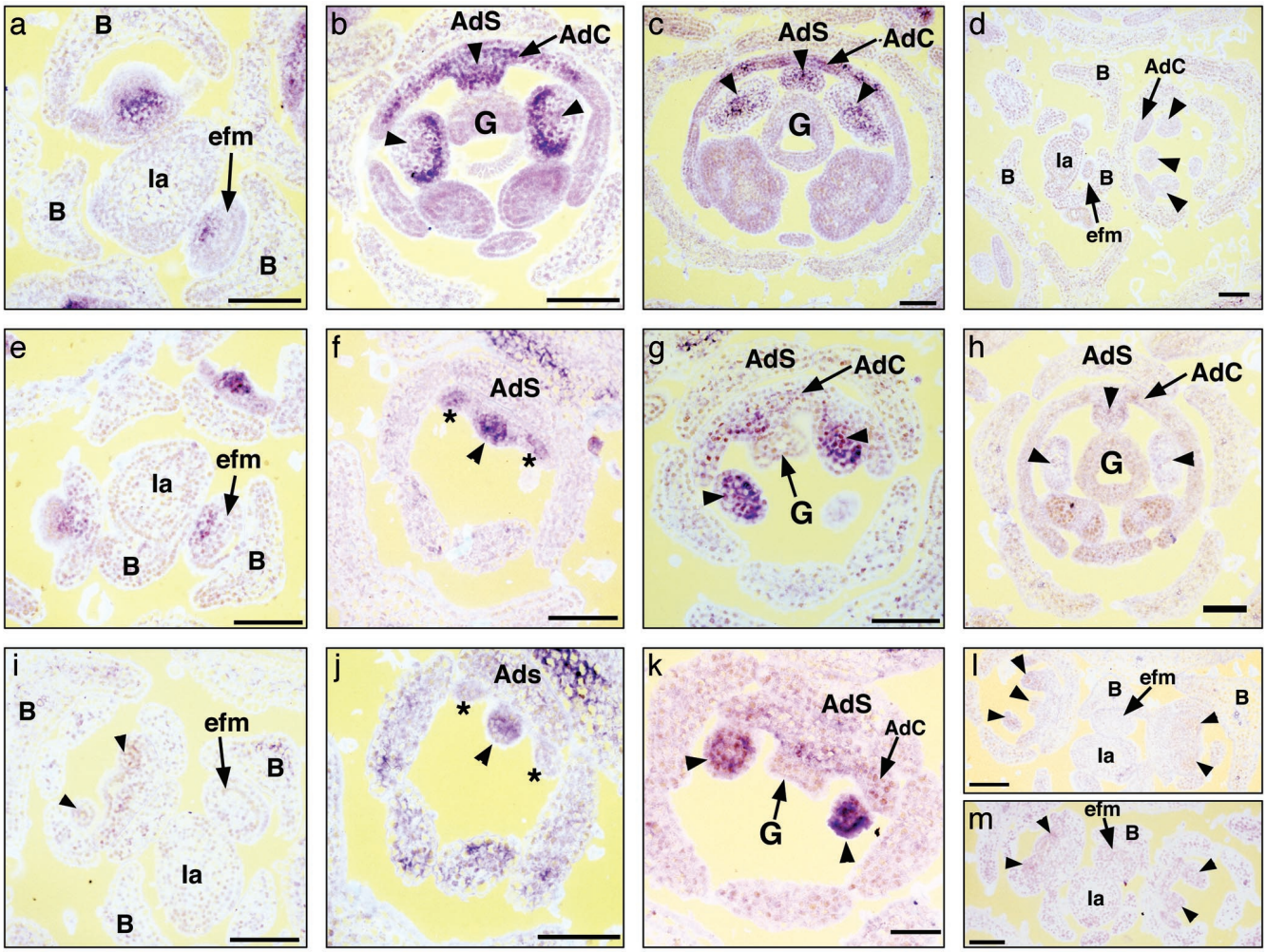

Fig. 4. Observed patterns of mRNA *in situ* hybridization in developing *M. confertiflora* flower meristems. (*a–c*) *McCYC1* antisense probe hybridized to *M. confertiflora* early through later stage flowers. (*a*) Transverse section through inflorescence; *McCYC1* expression is detected in the adaxial region of early floral meristems. (*b* and *c*) Transverse sections through mid-stage (*b*) and later stage (*c*) flowers; *McCYC1* expression is detected in adaxial and lateral staminodes and across the adaxial corolla. *McCYC2* expression patterns are identical to those of *McCYC1* across all observed stages of flower development (data not shown). (*d*) *McCYC1* sense probe hybridized to *M. confertiflora* flowers. (*e–h*) *McDICH1* antisense probe hybridized to *M. confertiflora* early through later stage flowers. (*e*) Transverse section through inflorescence; *McDICH1* expression is detected in the adaxial region of early floral meristems. (*f*) Oblique section through early stage flower; *McDICH1* expression is detected in the adaxial staminode and the adaxial petal primordia. (*g*) Oblique section through mid-stage flower; *McDICH1* expression is detected in the lateral staminodes but not in the adaxial petals. (*h*) Transverse section through later stage flower; *McDICH1* expression is not detected. (*i–k*) *McDICH2* antisense probe hybridized to *M. confertiflora* early through mid-stage flowers. (*i*) Transverse section through inflorescence; *McDICH2* expression is not detected in early floral meristems. (*j*) Oblique section through early stage flower; *McDICH2* expression is detected in the adaxial staminode but not in the adaxial petal primordia. (*k*) Oblique section through mid-stage flower; *McDICH2* expression is detected in the lateral staminodes but not in the adaxial petals. (*l* and *m*) *McDICH1* and *McDICH2* sense probes, respectively, hybridized to *M. confertiflora* flowers. (Scale bars, 100 μm.) Arrowheads indicate position of adaxial and lateral staminodes; asterisks indicate position of adaxial petal primordia; B, bract; la, inflorescence axis; efm, early floral meristem; G, gynoecium; AdS, adaxial sepal; AdC, adaxial corolla.

of adaxial petals at low levels, then the higher degree of internal adaxial petal symmetry in *Mohavea* may be due to the decrease in *McDICH* expression or to changes in downstream genes involved in cell division and expansion. In any case, alterations to the *DICH* pathway affecting adaxial petal morphology in *Mohavea* were likely only a single component of multiple evolutionary modifications to gene function and/or expression that resulted in the superficially actinomorphic appearance of *Mohavea* corollas.

Although the data do not allow identification of the specific mutations responsible for the derived flower morphology of *Mohavea*, they suggest that the effects of these mutations were partially mediated through the developmental control of adaxial flower identity, specifically, changes in the expression of the adaxial identity genes *CYC* and *DICH*. In the petal whorl, potential reduction in *McDICH* expression across adaxial petals may have evolved through cis- or trans-regulatory modifications. Because both *McCYC* and *McDICH* genes are expressed in *Mohavea* lateral stamen primordia, it is possible that changes in the cis-regulatory sequences of *McCYC1*, *McCYC2*, *McDICH1*, and *McDICH2* have resulted in their expanded expression. However, this explanation would require four separate cis-regulatory changes. More parsimoniously, changes in the expression domain of an upstream regulator in the *CYC/DICH* pathway may be responsible for alterations in *McCYC/McDICH* expression in the stamen whorl of the *Mohavea* lineage.

The *cyc* mutant phenotype in *A. majus* was described by Carpenter and Coen (26) as homeotic in nature, in that the

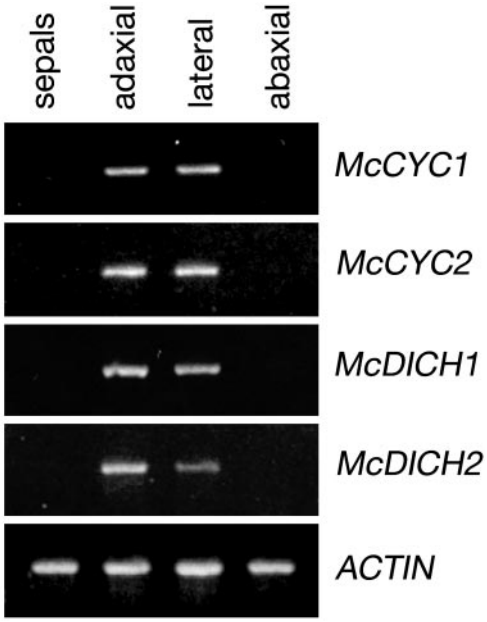

Fig. 5. Gene-specific RT-PCRs on RNA prepared from dissected *M. confertiflora* flower buds. Adaxial, lateral, and abaxial corolla and connate (attached) stamens were dissected from later stage buds (Fig. 1e). Sepal tissue was used as a negative control of *CYC* and *DICH* expression. Actin primers were used as a positive control. Locus specificity was confirmed by sequence analysis of RT-PCR products.

adaxial regions of flowers took on abaxial identity. Although homeotic mutations are generally studied within individual species, it has become widely accepted that homeotic-like transformations may play an important role in establishing morphological diversity (27–29). Shifts in gene expression correlated with such homeotic-like morphological transformations have been well documented in arthropods (30–33). Lateral stamen abortion in *Mohavea* can similarly be considered a homeotic-like transformation whereby lateral stamens have acquired adaxial identity, which in this case leads to abortion. We have established a strong correlation between expansion in the expression of the floral symmetry genes *CYC* and *DICH* into regions of lateral stamens and the ultimate abortion of these organs. Cubas *et al.* (9) have elegantly demonstrated that epigenetic mutations at the *CYC* locus are responsible for radially symmetrical mutants in populations of *Linaria vulgaris*. Although this phenotype can be considered a homeotic-like transformation, no evidence exists that such phenotypes contribute to interspecific differences in this group. Therefore, the expression of *CYC* and *DICH* in *Mohavea* represents the first clear correlation between changes in gene expression and homeotic-like evolutionary transformations in angiosperms.

Our observations provide direct evidence that major changes in floral morphology between species, including a homeotic-like transformation, are associated with changes in the regulation of floral symmetry gene expression. One critical aspect of this study is that the genetic basis for evolutionary changes in flower form can be linked to the ecological context in which the novel flower morphology arose. It is therefore important to ask whether adaptive significance can be attached to the derived features of *Mohavea* flowers and, thus, whether natural selection might have played a role in the observed evolutionary changes in *CYC* and *DICH* regulation. Whereas most *Antirrhinum* are specialized for pollination by nectar-foraging bees (21), *Mohavea* is unusual in being pollinated exclusively by pollen-collecting bees (22, 23). Furthermore, it appears that *M. confertiflora* is a floral mimic of the distantly related, but co-occurring, *Mentzelia involucrata* (Loasaceae) (23). *M. involucrata* flowers have radially symmetrical corollas and provide a large pollen reward to bees (22, 24). These pollen-collecting bees are the only known visitors to *M. confertiflora* flowers even though they provide minimal pollen reward (22, 23). Selection in *Mohavea* for mimetic similarity to *M. involucrata* likely favored mutations that enhance the actinomorphic appearance of the corolla. A component of the genetic changes leading to enhanced actinomorphy likely included the reduction of *McDICH* expression in the medial part of *Mohavea* adaxial petals. Likewise, the loss of lateral stamens may also be associated with the shift to pollen-collecting bees. Reduction in *Mohavea* stamen number is correlated with a change in abaxial anther position and pollen consistency. Together, these changes in stamen number and morphology are likely to reduce pollen loss to grooming after *Mohavea* flowers are visited by the pollen-collecting bee specialist (25). Although further ecological work is clearly needed (e.g., studies of how pollen-collecting bees respond to actinomorphic vs. zygomorphic flowers and further studies of pollen loss to grooming), it is clear that an integrative approach that bridges ecology, genetics, and development (34) has the potential to greatly improve our understanding of the mechanisms for adaptive evolution.

We thank Andrew Hudson for help with *in situ* protocols and Justin Blumenstiel, Colin Meiklejohn, Kristina Niovi Jones, Vivian Irish, and three anonymous reviewers for comments on early versions of this manuscript. Scanning electron microscopy images were kindly provided by Peter Endress. *M. confertiflora* seeds were kindly provided by the Rancho Santa Anna Botanical Garden seed program. North American *Antirrhinum* tissues were kindly provided by Ryan Oyama. Field-collected bee pollinators were identified as to species by Robbin Thorp. This work was funded by National Science Foundation Grant DEB-9972647 (to D.A.B. and L.C.H.).

1. Baum, D. A. (2002) in *Developmental Genetics and Plant Evolution*, eds. Cronk, Q. C. B., Bateman, R. M. & Hawkins, J. A. (Taylor and Francis, London), pp. 493–507.
2. Haag, E. S. & True, J. R. (2001) *Evolution (Lawrence, Kans.)* **55,** 1077–1084.
3. Endress, P. K. (1998) *Symp. Soc. Exp. Biol.* **51,** 133–140.
4. Luo, D., Carpenter, R., Copsey, L., Vincent, C., Clark, J. & Coen, E. (1999) *Cell* **99,** 367–376.
5. Luo, D., Carpenter, R., Vincent, C., Copsey, L. & Coen, E. (1996) *Nature* **383,** 794–799.
6. Rolland-Lagan, A. G., Bangham, J. A. & Coen, E. (2003) *Nature* **422,** 161–163.
7. Cubas, P., Lauter, N., Doebley, J. & Coen, E. (1999) *Plant J.* **18,** 215–222.
8. Doebley, J. F., Stec, A. & Hubbard, L. (1997) *Nature* **386,** 485–488.
9. Cubas, P., Vincent, C. & Coen, E. (1999) *Nature* **401,** 157–161.
10. Gillies, A. C. M., Cubas, P., Coen, E. S. & Abbott, R. J. (2002) in *Developmental Genetics and Plant Evolution*, eds. Cronk, Q. C. B., Bateman, R. M. & Hawkins, J. A. (Taylor and Francis, London), pp. 233–246.
11. Citerne, H. L., Moller, M. & Cronk, Q. C. B. (2000) *Ann. Bot.* **86,** 167–176.
12. Hileman, L. C. & Baum, D. A. (2003) *Mol. Biol. Evol.* **20,** 591–600.
13. Yang, Z. (1994) *J. Mol. Evol.* **39,** 306–314.
14. Yang, Z. (1994) *J. Mol. Evol.* **39,** 105–111.
15. Felsenstein, J. (1985) *Evolution (Lawrence, Kans.)* **39,** 783–791.
16. Swofford, D. L. (2001) PAUP*: Phylogenetic Analysis Using Parsimony (*and other methods) (Sinauer, Sunderland, MA), Version 4.0b1.
17. Lincoln, C., Long, J., Yamaguchi, J., Serikawa, K. & Hake, S. (1994) *Plant Cell* **6,** 1859–1876.
18. Kramer, E. M., Di Stilio, V. S. & Schluter, P. M. (2003) *Int. J. Plant Sci.* **164,** 1–11.
19. Prasad, K., Sriram, P., Kumar, C. S., Kushalappa, K. & Vijayraghavan, U. (2001) *Dev. Genes Evol.* **211,** 281–290.
20. Sutton, D. A. (1988) *A Revision of the Tribe Antirrhineae* (Oxford Univ. Press, Oxford).
21. Kampny, C. M. (1995) *Bot. Rev.* **61,** 350–366.
22. Snelling, R. R. & Stage, G. I. (1995) *Contrib. Sci./Nat. Hist. Museum Los Angeles County* **451,** 1–17.
23. Little, R. J. (1983) in *Handbook of Experimental Pollination Biology*, eds. Jones, C. E. & Little, R. J. (Van Nostrand Reinhold, New York), pp. 294–309.
24. Zavortink, T. J. (1972) *Proc. Entomol. Soc. Wash.* **74,** 61–75.

25. Harder, L. D. & Wilson, W. G. (1997) *Acta Hortic.* **437,** 83–101.
26. Carpenter, R. & Coen, E. (1990) *Genes Dev.* **4,** 1483–1493.
27. Carroll, S. B. (1995) *Nature* **376,** 479–485.
28. Hughes, C. L. & Kaufman, T. C. (2002) *Evol. Dev.* **4,** 459–499.
29. Browne, W. E. & Patel, N. H. (2000) *Semin. Cell Dev. Biol.* **11,** 427–435.
30. Averof, M. & Patel, N. H. (1997) *Nature* **388,** 682–686.
31. Abzhanov, A. & Kaufman, T. C. (1999) *Development (Cambridge, U.K.)* **126,** 1121–1128.
32. Abzhanov, A. & Kaufman, T. C. (2000) *Development (Cambridge, U.K.)* **127,** 2239–2249.
33. Abzhanov, A. & Kaufman, T. C. (2000) *Evol. Dev.* **2,** 271–283.
34. Givnish, T. J. (2003) *Taxon* **53,** 273–296.